

# Siliconated Pyrolytic Graphite

## Part 4 *Electrical Resistivity*

SEISHI YAJIMA, TOSHIO HIRAI

*Research Institute for Iron, Steel and Other Metals, Tohoku University, Sendai, Japan*

Received 3 February 1969

Investigations have been made on the electrical resistivity  $\rho$  of siliconated pyrolytic graphite (PG(Si), 0.02 to 4 wt % silicon) prepared by pyrolysis of a mixture of propane gas and silicon tetrachloride vapour at various deposition temperatures, total gas pressures, and partial pressures of silicon tetrachloride vapour. With increase in the partial pressure of silicon tetrachloride,  $\rho_a$  decreases and  $\rho_c$  increases. The electrical anisotropy ( $\rho_c/\rho_a$ ) of PG(Si) is two orders of magnitude higher than that of PG, at deposition temperatures between 1600 and 1700° C and a total gas pressure of 50 torr. Effects of the silicon content, density and structural features on the resistivities and the anisotropy have been discussed. The anisotropy is closely related to the preferred orientation, and high values of  $\rho_c/\rho_a$  induced by discontinuity in the stacking of crystallites are lowered in silicon-rich PG(Si) by the presence of SiC between the crystallites.

### 1. Introduction

Pyrolytic graphite (PG) tends to grow with its basal plane parallel to the substrate surface (deposition surface). X-ray analysis reveals varying degrees of preferred orientation. Since each crystallite has some anisotropic features reflecting the basic graphite structure, the preferred orientation is expected to transfer the intrinsic crystallite anisotropy to the bulk properties. The electrical anisotropy ( $\rho_c/\rho_a$ ) of PG measured in the parallel ( $\rho_a$ ) and perpendicular ( $\rho_c$ ) directions to the deposition surface is  $10^0$  to  $10^4$  [1-5]; the ratio is closely related to the structural features of PG, such as the preferred orientation [6], which depend on the preparation conditions [7, 8].

The electrical properties of PG-lamellar compounds (made by diffusing solutes into graphite) have been examined by Blackman *et al* [9]. On the other hand, Klein [5] investigated the electrical properties of boron-doped pyrolytic graphite, PG(B) (a PG-deposited compound made by co-depositing graphite and boron), and reported that  $\rho_a$  and  $\rho_c$  decreased with the boron content up to 0.6 wt %. Except for PG(B), there seem to have been no publications on the resistivities of PG-deposited compounds.

As reported in our previous papers [10-12], we prepared siliconated pyrolytic graphite (PG(Si)) containing up to 4 wt % silicon, and examined its microstructure, density and structural features. The object of this paper is to

TABLE I The preparation conditions of siliconated pyrolytic graphite, PG(Si)

Heating method	direct heating of substrate
Raw gas	propane gas + silicon tetrachloride vapour
Deposition temperature ( $T_{dep}$ )	1440 to 2025° C
Deposition time	20 to 120 min
Total gas pressure ( $P_{total}$ )	10, 50 torr
Partial pressure of SiCl <sub>4</sub> ( $P_{SiCl_4}$ )	0 to 13 torr

TABLE II Structural characteristics of the PG(Si) specimens

Silicon content (wt %)	0.02 to 4
Density (g/cm <sup>3</sup> )	1.4 to 2.22
Interlayer spacing (Å)	6.75 to 6.95
Preferred orientation, $\beta^*$ (deg)	20 to 36
Crystallite size, $L_a$ (Å)	60 to 2000
Crystallite size, $L_c$ (Å)	50 to 200

\*See [16, 17].

report the resistivities of PG(Si), especially with respect to the relations between the resistivities and the structural features.

**2. Experimental Procedures**

The process used for preparing PG(Si) samples was fully described in the first paper of this series [10]. Therefore, a simple description of the preparation conditions is included in table I. The basic characteristics of PG and PG(Si) samples used in this experiment are listed in table II. Resistivity measurements were also performed on samples which had been prepared by an indirect heating method at deposition temperatures between 1700 and 2300° C. As these samples were supplied by Nippon Carbon Co, they are indicated hereafter by the abbreviation "N".

For the resistivity determinations a current of about 0.05 to 0.2 A was passed through the specimen and a standard resistance connected in series. A simple four-point apparatus and a standard potentiometric method were used. Parasitic thermal effects were minimised by taking all the readings with normal and reversed currents. The resistivity measurements were carried out at 25° C. Since the resistivity in the *a*-direction varies depending on the sample thickness [13], samples less than 0.2 mm in thickness were employed for the resistivity measurements.

**3. Results and Discussions**

**3.1. Resistivity in the *a*-Direction,  $\rho_a$**

The effect of  $P_{SiCl_4}$  on  $\rho_a$  for PG(Si) samples

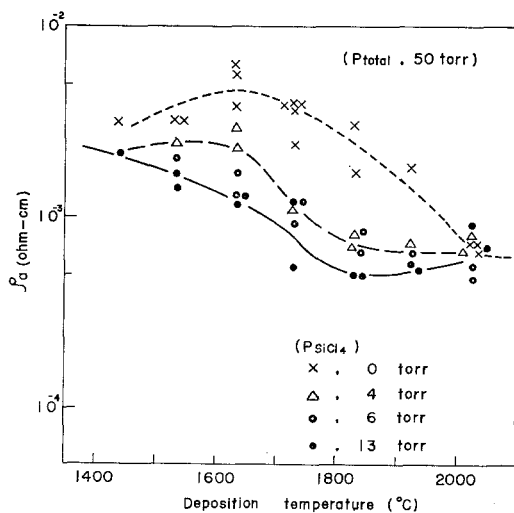


Figure 1 Effect of  $P_{SiCl_4}$  on the *a*-direction resistivity ( $\rho_a$ ) at  $P_{total} = 50$  torr.

prepared under various conditions is shown in figs. 1 and 2.

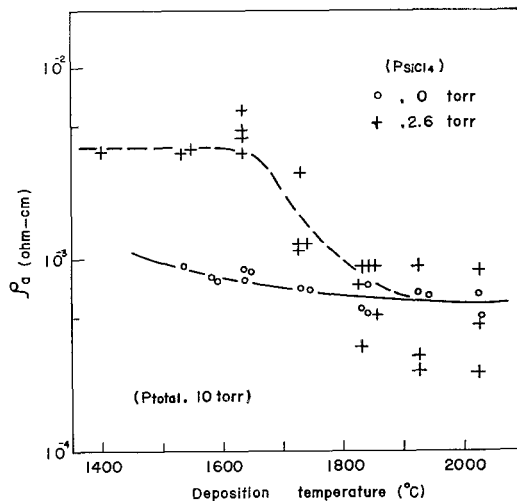


Figure 2 Effect of  $P_{SiCl_4}$  on  $\rho_a$  at  $P_{total} = 10$  torr.

Fig. 1 was obtained at  $P_{total} = 50$  torr, in which the broken line represents the results obtained at  $P_{SiCl_4} = 0$  torr. The dashed and full lines show the results at  $P_{SiCl_4} = 4$  and 13 torr respectively. At the deposition temperatures of 1400 and 2000° C, the values of  $\rho_a$  for PG(Si) are equal to those for PG. In the temperature range of 1500 to 1900° C, however,  $\rho_a$  for PG(Si) is smaller than that for PG and decreases with increasing  $P_{SiCl_4}$ .

Fig. 2 shows the relation of  $\rho_a$  to temperature at  $P_{total} = 10$  torr. Below 1800° C,  $\rho_a$  for PG(Si) is smaller than that for PG. At  $P_{total} = 10$  torr,  $\rho_a$  for PG(Si) is almost independent of tempera-

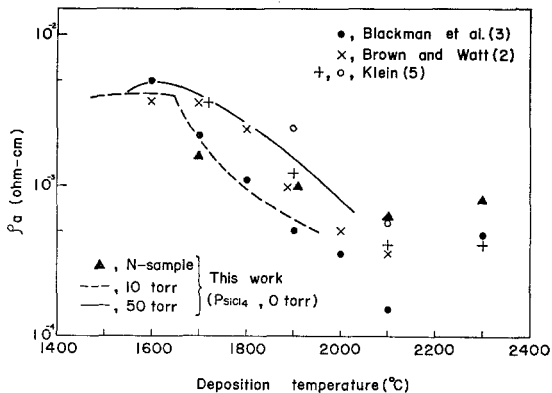


Figure 3 The value of  $\rho_a$  versus temperature, for PG.

ture and shows the values of  $8$  to  $6 \times 10^{-4} \Omega\text{cm}$  in the temperature range examined.

The values of  $\rho_a$  for PG( $P_{\text{SiCl}_4} = 0$  torr) are shown in fig. 3, which also includes the values obtained previously by other workers [2,3,5]. In fig. 3, the full and dashed lines represent the results at  $P_{\text{total}} = 50$  torr (fig. 1) and 10 torr (fig. 2), respectively. The value of  $\rho_a$  for the graphite single crystal is  $4.0 \times 10^{-5} \Omega\text{cm}$  [14]. The difference in the data shown in fig. 3 may be attributed to the preparation conditions employed.

### 3.2. Resistivity in the c-Direction, $\rho_c$

The effect of  $P_{\text{SiCl}_4}$  on  $\rho_c$  for PG(Si) is shown in figs. 4 and 5.

As shown in fig. 4, at  $P_{\text{total}} = 50$  torr,  $\rho_c$  is markedly affected by the addition of silicon tetrachloride vapour. A minimum value of  $\rho_c$  is observed for PG at 1600 to 1700° C, but not for PG(Si) in the temperature range examined. The temperature-dependence of  $\rho_c$  is similar to that of density [10]. At about 1700° C,  $\rho_c$  for PG(Si) is at least one order of magnitude higher than that for PG. For PG(Si),  $\rho_c$  is independent of  $P_{\text{SiCl}_4}$  above 1700° C. Below this temperature, however,

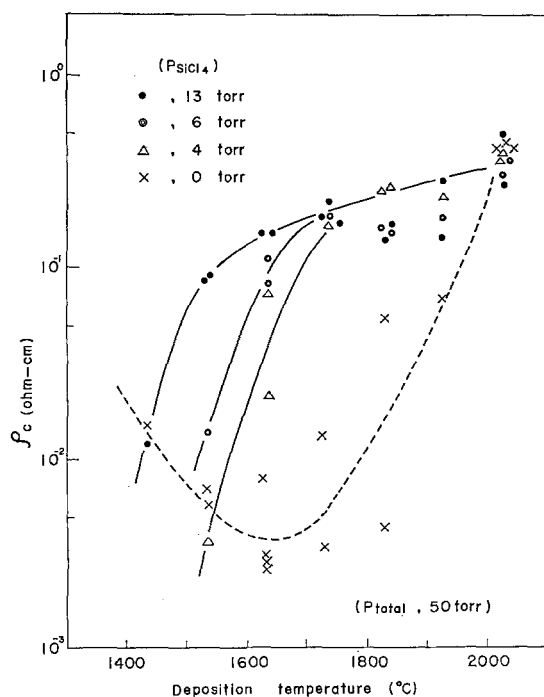


Figure 4 Effect of  $P_{\text{SiCl}_4}$  on the c-direction resistivity ( $\rho_c$ ) at  $P_{\text{total}} = 50$  torr.

$\rho_c$  depends on  $P_{\text{SiCl}_4}$  and increases with increasing  $P_{\text{SiCl}_4}$ .

In fig. 5, the relation at  $P_{\text{total}} = 10$  torr is given. Above 1800° C,  $\rho_c$  for PG(Si) is equal to that of PG. Below this temperature,  $\rho_c$  for PG(Si) is higher than that for PG.

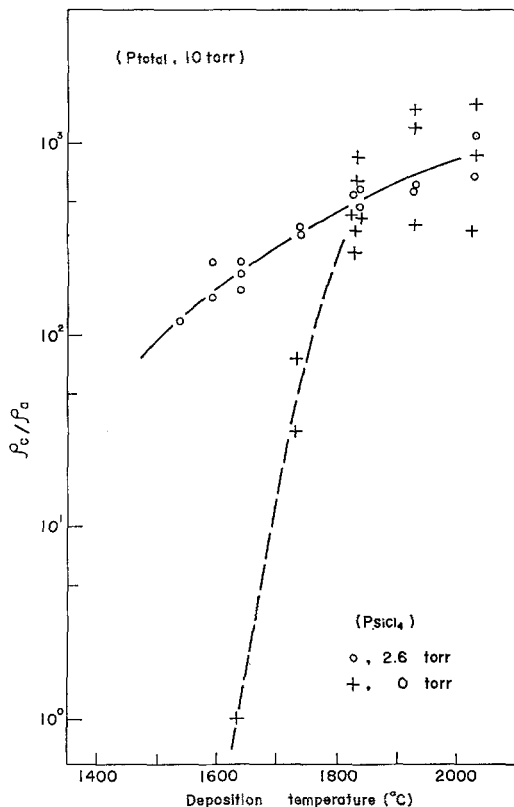


Figure 5 Effect of  $P_{\text{SiCl}_4}$  on  $\rho_c$  at  $P_{\text{total}} = 10$  torr.

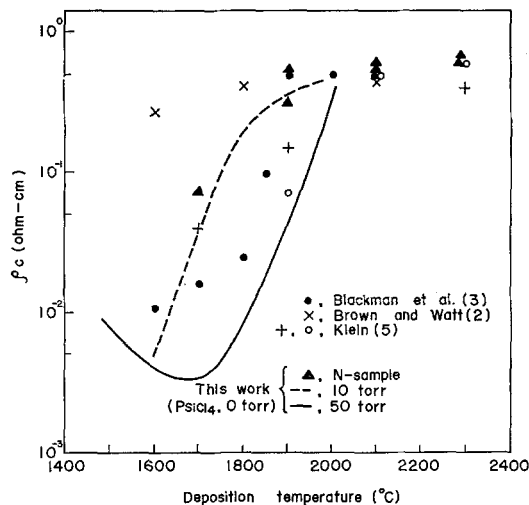


Figure 6 The value of  $\rho_c$  versus temperature, for PG.

The values of  $\rho_c$  for PG( $P_{SiCl_4} = 0$  torr) are shown in fig. 6, together with data in the literature [2, 3, 5]. In fig. 6, the full and dashed lines represent the results at  $P_{total} = 50$  torr (fig. 4) and 10 torr (fig. 5), respectively.

3.3. Electrical Anisotropy ( $\rho_c/\rho_a$ ) versus Deposition Temperature

The effect of  $P_{SiCl_4}$  on  $\rho_c/\rho_a$  for PG(Si) is shown in fig. 7 ( $P_{total} = 50$  torr) and fig. 8 ( $P_{total} = 10$  torr).

As shown in fig. 7, at  $P_{total} = 50$  torr,  $\rho_c/\rho_a$  for PG(Si) is equal to that for PG ( $\sim 5 \times 10^2$ ) at  $2000^\circ C$ . However, at  $1600$  to  $1700^\circ C$ ,  $\rho_c/\rho_a$  for PG(Si) is two orders of magnitude higher than that for PG.

Fig. 8 was obtained at  $P_{total} = 10$  torr, in which  $\rho_c/\rho_a$  is  $5 \times 10^2 - 1 \times 10^3$  for PG and PG(Si) above  $1800^\circ C$ . In the low temperature range below  $1800^\circ C$ ,  $\rho_c/\rho_a$  for PG(Si) is higher than that for PG.

The values of  $\rho_c/\rho_a$  for PG( $P_{SiCl_4} = 0$  torr) are summarised in fig. 9. As shown in the figure,  $\rho_c/\rho_a$  increases with increasing temperature from

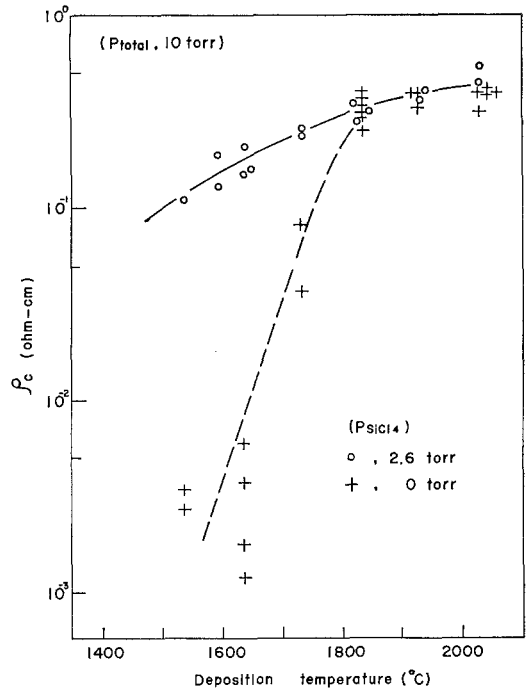


Figure 8 Effect of  $P_{SiCl_4}$  on  $\rho_c/\rho_a$  at  $P_{total} = 10$  torr.

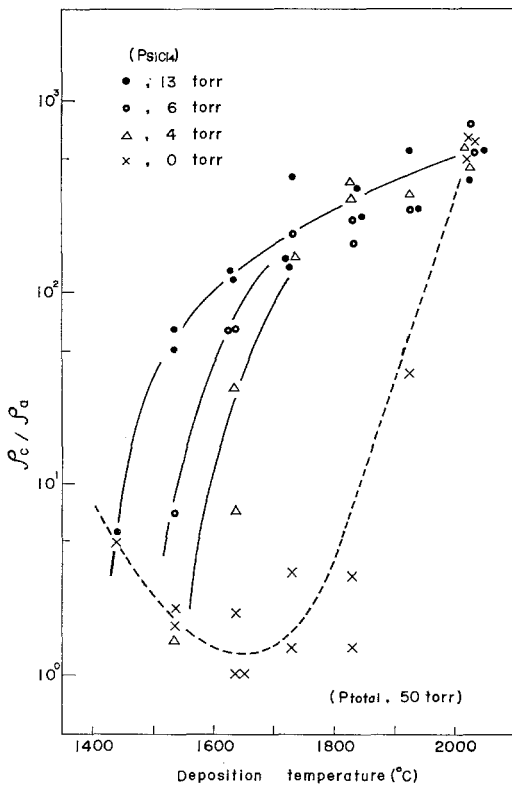


Figure 7 Effect of  $P_{SiCl_4}$  on the electrical anisotropy ( $\rho_c/\rho_a$ ) at  $P_{total} = 50$  torr.

$10^0$  to  $10^3$  in the temperature range of  $1600$  to  $2000^\circ C$ , and is constant ( $\sim 1 \times 10^3$ ) above  $2000^\circ C$ .

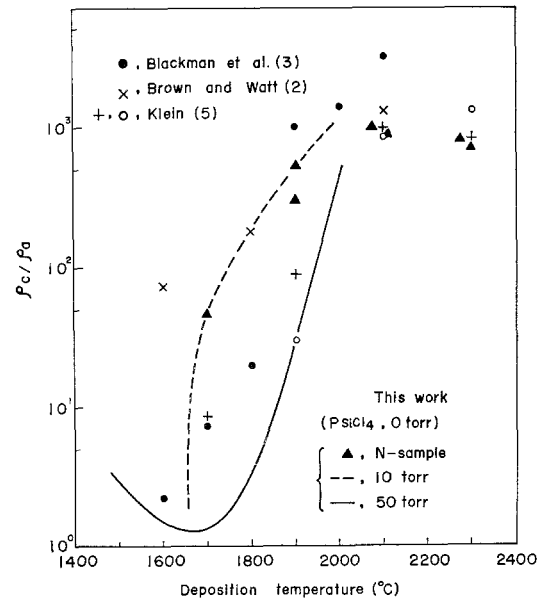


Figure 9 The value of  $\rho_c/\rho_a$  versus temperature, for PG.

### 3.4. Variation in Resistivity with Silicon Content

Klein [5] studied the effect of the boron content on the resistivities of PG(B). In the present experiment, it was impossible to prepare the PG(Si) of different silicon contents while retaining the same structural features of its graphite matrix, as discussed in the previous paper [12]. Therefore, the effect of silicon content on the resistivities cannot be examined here.

### 3.5. Variation in Resistivity with Density

Brown and Watt [2] plotted  $\rho_a$  against density ( $d$ ), and indicated the following relationship for PG samples prepared in the temperature range of 1700 to 2000° C:

$$\rho_a = \frac{\text{constant}}{d^3}.$$

However, in the present experiment, this relationship is not found, as shown in fig. 10. The values of  $\rho_a$  for PG samples having the same density, prepared at  $P_{\text{total}} = 50$  torr ( $T_{\text{dep}} > 1800^\circ\text{C}$ ) and  $P_{\text{total}} = 10$  torr ( $T_{\text{dep}} > 1600^\circ\text{C}$ ) respective-

ly, are different. This indicates that  $\rho_a$  depends strongly on the structural features rather than on the density. The differences between the relations for PG and PG(Si) seem to depend not on the silicon content but on the variation in the structural features.

### 3.6. Variation in Resistivity with Crystallite Size

Bowman *et al* [15] illustrated the correlation between  $\rho_a$  and  $L_a$  by plotting  $\rho_a$  against  $1/L_a$ , for several graphites, and proposed the following linear dependence:

$$\rho_a = \frac{R}{n_0 + AT} \left( \frac{1}{L_a} + \frac{1}{L_0} + BC_v \right).$$

Here,  $L_a$  = mean crystallite diameter;  $L_0$  = mean free path due to other fixed scattering centres; R, A, B = constants depending on band structure and scattering mechanism;  $C_v$  = specific heat;  $T$  = temperature;  $n_0$  = effective carrier density at absolute zero.

A linear relation was also obtained for PG and PG(Si) in this experiment. These results are shown in fig. 11. The difference in these gradients

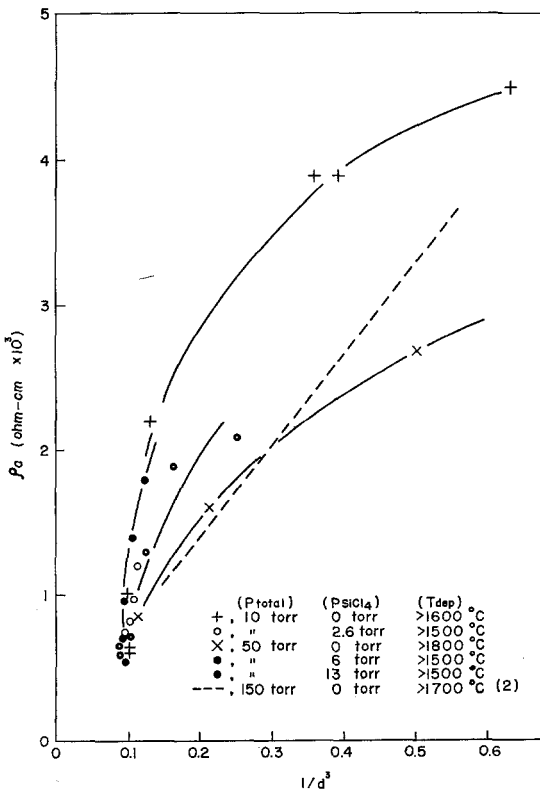


Figure 10 Relation between  $\rho_a$  and density ( $d$ ).

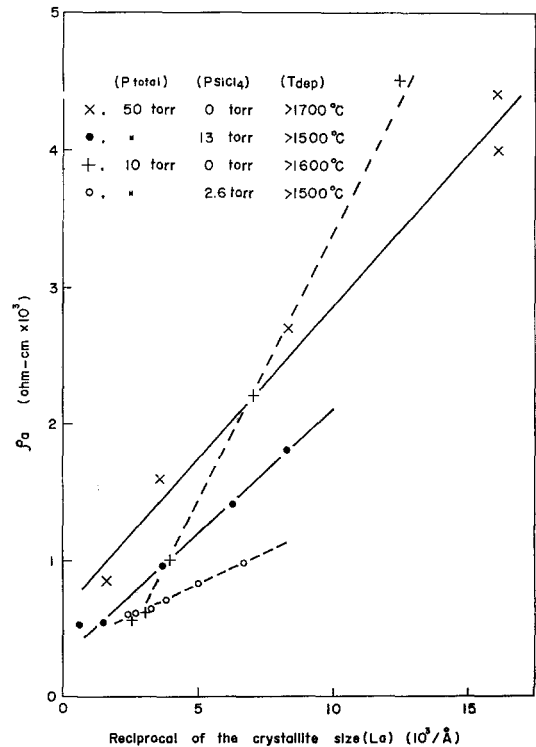


Figure 11 Relation between  $\rho_a$  and crystallite size ( $L_a$ ).

shows that  $\rho_a$  cannot always be interpreted in terms of the crystallite size alone.

### 3.7. Variation in Resistivity with Preferred Orientation

The relations between the preferred orientation and resistivities ( $\rho_a$  and  $\rho_c$ ) are shown in figs. 12 and 13, respectively. As shown in these figures,  $\rho_a$  decreases and  $\rho_c$  increases with increasing degree of the preferred orientation (corresponding to decreasing  $\beta$ ). Fig. 14 shows the relation

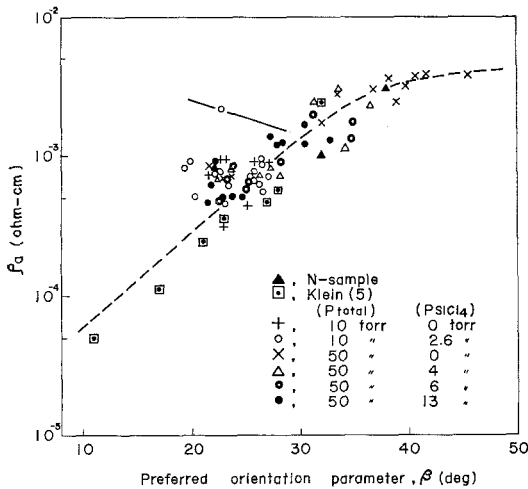


Figure 12 Relation between  $\rho_a$  and preferred orientation parameter ( $\beta$ ). The deviating point has a high silicon content.

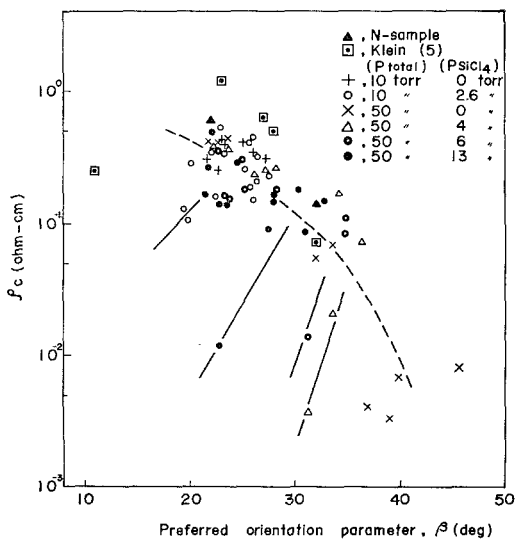


Figure 13 Relation between  $\rho_c$  and  $\beta$ . The deviating points have high silicon contents.

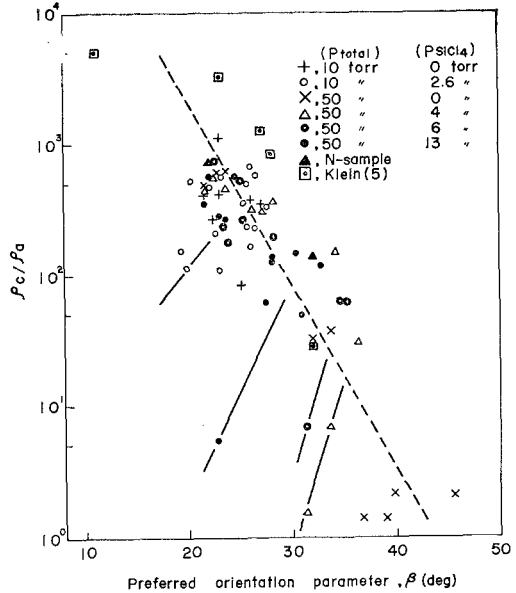


Figure 14 Relation between  $\rho_c/\rho_a$  and  $\beta$ . The deviating points have high silicon contents.

between  $\rho_c/\rho_a$  and the preferred orientation, from which it is evident that  $\rho_c/\rho_a$  is closely related to  $\beta$ . These figures include the data after Klein [5]. In figs. 12 to 14, the points remote from the dashed line (linked to it by solid lines) indicate the results obtained on the PG(Si) samples containing large amounts of silicon.

Guentert and Klein [6] examined the correlation between the preferred orientation and  $\rho_c/\rho_a$ , and proposed the following equation:

$$\frac{\rho_c}{\rho_a} = \frac{(m + 2) \rho_{1c}/\rho_{1a} + 1}{2 \rho_{1c}/\rho_{1a} + (m + 1)},$$

where  $\rho_c/\rho_a$  is the bulk (effective, measured) anisotropy and  $\rho_{1c}/\rho_{1a}$  is the crystallite (intrinsic) anisotropy, and  $m$  is the preferred orientation index.

Since  $\beta = 1.18 m^{-1/2}$  [16, 17], we obtain

$$\frac{\rho_c}{\rho_a} = \frac{(1.4/\beta^2 + 2) \rho_{1c}/\rho_{1a} + 1}{2 \rho_{1c}/\rho_{1a} + (1.4/\beta^2 + 1)},$$

where  $\beta$  is in radians. When  $\rho_{1c}/\rho_{1a} = 10^2$  to  $10^4$  ( $10^2$  to  $10^4$  for the graphite single crystal), the calculated variation of  $\rho_c/\rho_a$  with  $\beta$  is shown by the full line in fig. 15. The dashed line represents the result shown in fig. 14. Fig. 15 shows that  $\rho_c/\rho_a$  for PG cannot be accounted for exclusively in terms of crystallite orientation. According to the interpretation by Guentert and Klein, it seems reasonable to attribute the unusually high

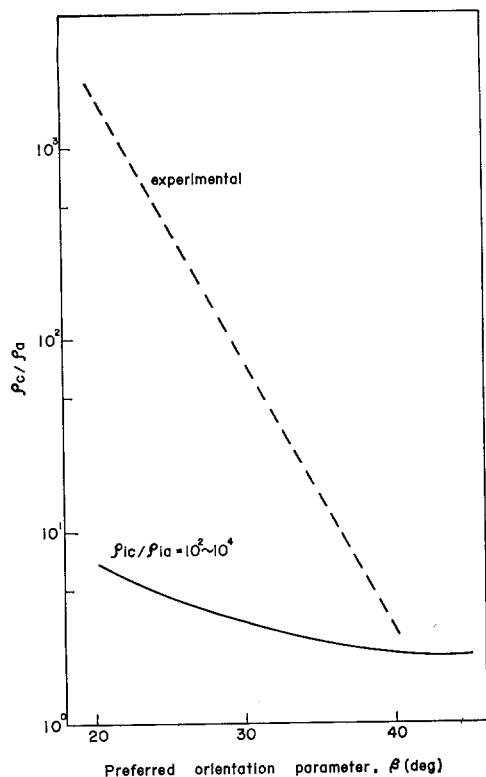


Figure 15 Calculated crystallite electrical anisotropy ( $\rho_c/\rho_a$ ) and experimental bulk electrical anisotropy ( $\rho_c/\rho_a$ ).

values of  $\rho_c/\rho_a$  to the anomalous  $c$ -direction flow conditions, induced by discontinuity in the stacking of the wrinkled sheets. For the PG(Si) samples containing large amounts of silicon, however, this discontinuity disappears because of the presence of SiC between the crystallites, as reported in a previous paper [11]. This explains why (as indicated by the deviating points of fig. 14) ( $\rho_c/\rho_a$ ) of PG(Si) decreases with increasing silicon content.

#### 4. Conclusions

(i) The resistivities ( $\rho_a$  and  $\rho_c$ ) of PG(Si) are strikingly affected by the addition of silicon tetrachloride, below 2000° C at  $P_{\text{total}} = 50$  torr, and below about 1800° C at  $P_{\text{total}} = 10$  torr. With increasing  $P_{\text{SiCl}_4}$ ,  $\rho_a$  decreases and  $\rho_c$  increases.

(ii) The electrical anisotropy ( $\rho_c/\rho_a$ ) of PG(Si) is two orders of magnitude higher than that of PG in the temperature range of 1600 to 1700° C ( $P_{\text{total}} = 50$  torr).

(iii) The variations in resistivity with silicon content and density are not clear.

(iv) The relation between  $\rho_a$  and  $1/L_a$  shows a linear dependence. However, the linear relation does not provide decisive information on the resistivities of PG and PG(Si).

(v) The electrical anisotropy is closely related to the preferred orientation. High values of  $\rho_c/\rho_a$  induced by discontinuity in the stacking of crystallites are lowered by the presence of SiC between the crystallites for the PG(Si) samples containing large amounts of silicon.

#### Acknowledgement

The authors wish to express their appreciation to Mr Yoshiharu Chiba (Tohoku University) for his assistance in the preparation of various specimens, and also to Nippon Carbon Co for supplying the pyrolytic graphite samples ("N").

#### References

1. A. R. G. BROWN, W. WATT, R. W. POWELL, and R. P. TYE, *Brit. J. Appl. Phys.* **7** (1956) 73.
2. A. R. G. BROWN and W. WATT, Proc. Conf. on Carbon and Graphite (Soc. Chem. Ind., London, 1958) p. 86.
3. L. C. BLACKMAN, G. SAUNDERS, and A. R. UBBELOHDE, *Proc. Roy. Soc. A* **264** (1961) 19.
4. A. R. UBBELOHDE, Proc. 5th Conf. Carbon (Pergamon Press, Oxford, 1962) p.1.
5. C. A. KLEIN, *J. Appl. Phys.* **33** (1962) 3338; *Rev. Mod. Phys.* **34** (1962) 56.
6. O. J. GUENTERT and C. A. KLEIN, *Appl. Phys. Lett.* **2** (1963) 125.
7. S. YAJIMA, T. SATOW, and T. HIRAI, *J. Nucl. Mats.* **17** (1965) 127.
8. T. HIRAI and S. YAJIMA, *J. Materials Sci.* **2** (1967) 18.
9. L. C. BLACKMAN, J. F. MATHEWS, and A. R. UBBELOHDE, *Proc. Roy. Soc. A* **256** (1960) 15; **A258** (1960) 329, 339.
10. S. YAJIMA and T. HIRAI, *J. Materials Sci.* **4** (1969) 416.
11. *Idem, ibid* 424.
12. *Idem, ibid* 685.
13. T. HIRAI, unpublished work.
14. W. PRIMAK and L. H. FUCHS, *Phys. Rev.* **95** (1954) 22.
15. J. C. BOWMAN, J. A. KRUMHANSL, and J. T. MEERS, Proc. Conf. on Carbon and Graphite (Soc. Chem. Ind., London, 1958) p. 52.
16. D. B. FISCHBACH, *J. Appl. Phys.* **37** (1966) 2202.
17. T. HIRAI, *ibid* **38** (1967) 902; *Trans. Japan Inst. Met.* **8** (1967) 190.